Measurements of branching fractions, polarizations, and direct CP-violation asymmetries in B(+) -> rho(0)K*(+) and B(+) -> f(0)(980)K*(+) decays

del Amo Sanchez, P.; Raven, H.G.; Snoek, H.

published in
Physical Review D
2011

DOI (link to publisher)
10.1103/PhysRevD.83.051101

document version
Publisher's PDF, also known as Version of record

PHYSICAL REVIEW D **83,** 051101(R) (2011)

Measurements of branching fractions, polarizations, and direct *CP*-violation asymmetries in $B^+ \to \rho^0 K^{*+}$ and $B^+ \to f_0(980) K^{*+}$ decays

P. del Amo Sanchez,[1] J. P. Lees,[1] V. Poireau,[1] E. Prencipe,[1] V. Tisserand,[1] J. Garra Tico,[2] E. Grauges,[2] M. Martinelli,[3a,3b] D. A. Milanes,[3a] A. Palano,[3a,3b] M. Pappagallo,[3a,3b] G. Eigen,[4] B. Stugu,[4] L. Sun,[4] D. N. Brown,[5] L. T. Kerth,[5] Yu. G. Kolomensky,[5] G. Lynch,[5] I. L. Osipenkov,[5] H. Koch,[6] T. Schroeder,[6] D. J. Asgeirsson,[7] C. Hearty,[7] T. S. Mattison,[7] J. A. McKenna,[7] A. Khan,[8] V. E. Blinov,[9] A. R. Buzykaev,[9] V. P. Druzhinin,[9] V. B. Golubev,[9] E. A. Kravchenko,[9] A. P. Onuchin,[9] S. I. Serednyakov,[9] Yu. I. Skovpen,[9] E. P. Solodov,[9] K. Yu. Todyshev,[9] A. N. Yushkov,[9] M. Bondioli,[10] S. Curry,[10] D. Kirkby,[10] A. J. Lankford,[10] M. Mandelkern,[10] E. C. Martin,[10] D. P. Stoker,[10] H. Atmacan,[11] J. W. Gary,[11] F. Liu,[11] O. Long,[11] G. M. Vitug,[11] C. Campagnari,[12] T. M. Hong,[12] D. Kovalskyi,[12] J. D. Richman,[12] C. West,[12] A. M. Eisner,[13] C. A. Heusch,[13] J. Kroseberg,[13] W. S. Lockman,[13] A. J. Martinez,[13] T. Schalk,[13] B. A. Schumm,[13] A. Seiden,[13] L. O. Winstrom,[13] C. H. Cheng,[14] D. A. Doll,[14] B. Echenard,[14] D. G. Hitlin,[14] P. Ongmongkolkul,[14] F. C. Porter,[14] A. Y. Rakitin,[14] R. Andreassen,[15] M. S. Dubrovin,[15] G. Mancinelli,[15] B. T. Meadows,[15] M. D. Sokoloff,[15] P. C. Bloom,[16] W. T. Ford,[16] A. Gaz,[16] M. Nagel,[16] U. Nauenberg,[16] J. G. Smith,[16] S. R. Wagner,[16] R. Ayad,[17,*] W. H. Toki,[17] H. Jasper,[18] T. M. Karbach,[18] A. Petzold,[18] B. Spaan,[18] M. J. Kobel,[19] K. R. Schubert,[19] R. Schwierz,[19] D. Bernard,[20] M. Verderi,[20] P. J. Clark,[21] S. Playfer,[21] J. E. Watson,[21] M. Andreotti,[22a,22b] D. Bettoni,[22a] C. Bozzi,[22a] R. Calabrese,[22a,22b] A. Cecchi,[22a,22b] G. Cibinetto,[22a,22b] E. Fioravanti,[22a,22b] P. Franchini,[22a,22b] I. Garzia,[22a,22b] E. Luppi,[22a,22b] M. Munerato,[22a,22b] M. Negrini,[22a,22b] A. Petrella,[22a,22b] L. Piemontese,[22a] R. Baldini-Ferroli,[23] A. Calcaterra,[23] R. de Sangro,[23] G. Finocchiaro,[23] M. Nicolaci,[23] S. Pacetti,[23] P. Patteri,[23] I. M. Peruzzi,[23,†] M. Piccolo,[23] M. Rama,[23] A. Zallo,[23] R. Contri,[24a,24b] E. Guido,[24a,24b] M. Lo Vetere,[24a,24b] M. R. Monge,[24a,24b] S. Passaggio,[24a] C. Patrignani,[24a,24b] E. Robutti,[24a] S. Tosi,[24a,24b] B. Bhuyan,[25] V. Prasad,[25] C. L. Lee,[26] M. Morii,[26] A. J. Edwards,[27] A. Adametz,[28] J. Marks,[28] U. Uwer,[28] F. U. Bernlochner,[29] M. Ebert,[29] H. M. Lacker,[29] T. Lueck,[29] A. Volk,[29] P. D. Dauncey,[30] M. Tibbetts,[30] P. K. Behera,[31] U. Mallik,[31] C. Chen,[32] J. Cochran,[32] H. B. Crawley,[32] L. Dong,[32] W. T. Meyer,[32] S. Prell,[32] E. I. Rosenberg,[32] A. E. Rubin,[32] A. V. Gritsan,[33] Z. J. Guo,[33] N. Arnaud,[34] M. Davier,[34] D. Derkach,[34] J. Firmino da Costa,[34] G. Grosdidier,[34] F. Le Diberder,[34] A. M. Lutz,[34] B. Malaescu,[34] A. Perez,[34] P. Roudeau,[34] M. H. Schune,[34] J. Serrano,[34] V. Sordini,[34,‡] A. Stocchi,[34] L. Wang,[34] G. Wormser,[34] D. J. Lange,[35] D. M. Wright,[35] I. Bingham,[36] C. A. Chavez,[36] J. P. Coleman,[36] J. R. Fry,[36] E. Gabathuler,[36] R. Gamet,[36] D. E. Hutchcroft,[36] D. J. Payne,[36] C. Touramanis,[36] A. J. Bevan,[37] F. Di Lodovico,[37] R. Sacco,[37] M. Sigamani,[37] G. Cowan,[38] S. Paramesvaran,[38] A. C. Wren,[38] D. N. Brown,[39] C. L. Davis,[39] A. G. Denig,[40] M. Fritsch,[40] W. Gradl,[40] A. Hafner,[40] K. E. Alwyn,[41] D. Bailey,[41] R. J. Barlow,[41] G. Jackson,[41] G. D. Lafferty,[41] J. Anderson,[42] R. Cenci,[42] A. Jawahery,[42] D. A. Roberts,[42] G. Simi,[42] J. M. Tuggle,[42] C. Dallapiccola,[43] E. Salvati,[43] R. Cowan,[44] D. Dujmic,[44] G. Sciolla,[44] M. Zhao,[44] D. Lindemann,[45] P. M. Patel,[45] S. H. Robertson,[45] M. Schram,[45] P. Biassoni,[46a,46b] A. Lazzaro,[46a,46b] V. Lombardo,[46a] F. Palombo,[46a,46b] S. Stracka,[46a,46b] L. Cremaldi,[47] R. Godang,[47,§] R. Kroeger,[47] P. Sonnek,[47] D. J. Summers,[47] X. Nguyen,[48] M. Simard,[48] P. Taras,[48] G. De Nardo,[49a,49b] D. Monorchio,[49a,49b] G. Onorato,[49a,49b] C. Sciacca,[49a,49b] G. Raven,[50] H. L. Snoek,[50] C. P. Jessop,[51] K. J. Knoepfel,[51] J. M. LoSecco,[51] W. F. Wang,[51] L. A. Corwin,[52] K. Honscheid,[52] R. Kass,[52] J. P. Morris,[52] N. L. Blount,[53] J. Brau,[53] R. Frey,[53] O. Igonkina,[53] J. A. Kolb,[53] R. Rahmat,[53] N. B. Sinev,[53] D. Strom,[53] J. Strube,[53] E. Torrence,[53] G. Castelli,[54a,54b] E. Feltresi,[54a,54b] N. Gagliardi,[54a,54b] M. Margoni,[54a,54b] M. Morandin,[54a] M. Posocco,[54a] M. Rotondo,[54a] F. Simonetto,[54a,54b] R. Stroili,[54a,54b] E. Ben-Haim,[55] G. R. Bonneaud,[55] H. Briand,[55] G. Calderini,[55] J. Chauveau,[55] O. Hamon,[55] Ph. Leruste,[55] G. Marchiori,[55] J. Ocariz,[55] J. Prendki,[55] S. Sitt,[55] M. Biasini,[56a,56b] E. Manoni,[56a,56b] A. Rossi,[56a,56b] C. Angelini,[57a,57b] G. Batignani,[57a,57b] S. Bettarini,[57a,57b] M. Carpinelli,[57a,57b,‖] G. Casarosa,[57a,57b] A. Cervelli,[57a,57b] F. Forti,[57a,57b] M. A. Giorgi,[57a,57b] A. Lusiani,[57a,57c] N. Neri,[57a,57b] E. Paoloni,[57a,57b] G. Rizzo,[57a,57b] J. J. Walsh,[57a] D. Lopes Pegna,[58] C. Lu,[58] J. Olsen,[58] A. J. S. Smith,[58] A. V. Telnov,[58] F. Anulli,[59a] E. Baracchini,[59a,59b] G. Cavoto,[59a] R. Faccini,[59a,59b] F. Ferrarotto,[59a] F. Ferroni,[59a,59b] M. Gaspero,[59a,59b] L. Li Gioi,[59a] M. A. Mazzoni,[59a] G. Piredda,[59a] F. Renga,[59a,59b] T. Hartmann,[60] T. Leddig,[60] H. Schröder,[60] R. Waldi,[60] T. Adye,[61] B. Franek,[61] E. O. Olaiya,[61] F. F. Wilson,[61] S. Emery,[62] G. Hamel de Monchenault,[62] G. Vasseur,[62] Ch. Yèche,[62] M. Zito,[62] M. T. Allen,[63] D. Aston,[63] D. J. Bard,[63] R. Bartoldus,[63] J. F. Benitez,[63] C. Cartaro,[63] M. R. Convery,[63] J. Dorfan,[63] G. P. Dubois-Felsmann,[63] W. Dunwoodie,[63] R. C. Field,[63] M. Franco Sevilla,[63] B. G. Fulsom,[63] A. M. Gabareen,[63] M. T. Graham,[63] P. Grenier,[63] C. Hast,[63] W. R. Innes,[63] M. H. Kelsey,[63] H. Kim,[63] P. Kim,[63] M. L. Kocian,[63] D. W. G. S. Leith,[63] S. Li,[63] B. Lindquist,[63] S. Luitz,[63] V. Luth,[63] H. L. Lynch,[63] D. B. MacFarlane,[63] H. Marsiske,[63] D. R. Muller,[63] H. Neal,[63] S. Nelson,[63] C. P. O'Grady,[63] I. Ofte,[63] M. Perl,[63] T. Pulliam,[63] B. N. Ratcliff,[63] A. Roodman,[63] A. A. Salnikov,[63] V. Santoro,[63] R. H. Schindler,[63] J. Schwiening,[63]

A. Snyder,[63] D. Su,[63] M. K. Sullivan,[63] S. Sun,[63] K. Suzuki,[63] J. M. Thompson,[63] J. Va'vra,[63] A. P. Wagner,[63] M. Weaver,[63] W. J. Wisniewski,[63] M. Wittgen,[63] D. H. Wright,[63] H. W. Wulsin,[63] A. K. Yarritu,[63] C. C. Young,[63] V. Ziegler,[63] X. R. Chen,[64] W. Park,[64] M. V. Purohit,[64] R. M. White,[64] J. R. Wilson,[64] A. Randle-Conde,[65] S. J. Sekula,[65] M. Bellis,[66] P. R. Burchat,[66] T. S. Miyashita,[66] S. Ahmed,[67] M. S. Alam,[67] J. A. Ernst,[67] B. Pan,[67] M. A. Saeed,[67] S. B. Zain,[67] N. Guttman,[68] A. Soffer,[68] P. Lund,[69] S. M. Spanier,[69] R. Eckmann,[70] J. L. Ritchie,[70] A. M. Ruland,[70] C. J. Schilling,[70] R. F. Schwitters,[70] B. C. Wray,[70] J. M. Izen,[71] X. C. Lou,[71] F. Bianchi,[72a,72b] D. Gamba,[72a,72b] M. Pelliccioni,[72a,72b] M. Bomben,[73a,73b] L. Lanceri,[73a,73b] L. Vitale,[73a,73b] N. Lopez-March,[74] F. Martinez-Vidal,[74] A. Oyanguren,[74] J. Albert,[75] Sw. Banerjee,[75] H. H. F. Choi,[75] K. Hamano,[75] G. J. King,[75] R. Kowalewski,[75] M. J. Lewczuk,[75] C. Lindsay,[75] I. M. Nugent,[75] J. M. Roney,[75] R. J. Sobie,[75] T. J. Gershon,[76] P. F. Harrison,[76] T. E. Latham,[76] E. M. T. Puccio,[76] H. R. Band,[77] S. Dasu,[77] K. T. Flood,[77] Y. Pan,[77] R. Prepost,[77] C. O. Vuosalo,[77] and S. L. Wu[77]

(The *BABAR* Collaboration)

[1]*Laboratoire d'Annecy-le-Vieux de Physique des Particules (LAPP), Université de Savoie, CNRS/IN2P3, F-74941 Annecy-Le-Vieux, France*
[2]*Universitat de Barcelona, Facultat de Fisica, Departament ECM, E-08028 Barcelona, Spain*
[3a]*INFN Sezione di Bari, I-70126 Bari, Italy*
[3b]*Dipartimento di Fisica, Università di Bari, I-70126 Bari, Italy*
[4]*University of Bergen, Institute of Physics, N-5007 Bergen, Norway*
[5]*Lawrence Berkeley National Laboratory and University of California, Berkeley, California 94720, USA*
[6]*Ruhr Universität Bochum, Institut für Experimentalphysik 1, D-44780 Bochum, Germany*
[7]*University of British Columbia, Vancouver, British Columbia, Canada V6T 1Z1*
[8]*Brunel University, Uxbridge, Middlesex UB8 3PH, United Kingdom*
[9]*Budker Institute of Nuclear Physics, Novosibirsk 630090, Russia*
[10]*University of California at Irvine, Irvine, California 92697, USA*
[11]*University of California at Riverside, Riverside, California 92521, USA*
[12]*University of California at Santa Barbara, Santa Barbara, California 93106, USA*
[13]*University of California at Santa Cruz, Institute for Particle Physics, Santa Cruz, California 95064, USA*
[14]*California Institute of Technology, Pasadena, California 91125, USA*
[15]*University of Cincinnati, Cincinnati, Ohio 45221, USA*
[16]*University of Colorado, Boulder, Colorado 80309, USA*
[17]*Colorado State University, Fort Collins, Colorado 80523, USA*
[18]*Technische Universität Dortmund, Fakultät Physik, D-44221 Dortmund, Germany*
[19]*Technische Universität Dresden, Institut für Kern- und Teilchenphysik, D-01062 Dresden, Germany*
[20]*Laboratoire Leprince-Ringuet, CNRS/IN2P3, Ecole Polytechnique, F-91128 Palaiseau, France*
[21]*University of Edinburgh, Edinburgh EH9 3JZ, United Kingdom*
[22a]*INFN Sezione di Ferrara, I-44100 Ferrara, Italy*
[22b]*Dipartimento di Fisica, Università di Ferrara, I-44100 Ferrara, Italy*
[23]*INFN Laboratori Nazionali di Frascati, I-00044 Frascati, Italy*
[24a]*INFN Sezione di Genova, I-16146 Genova, Italy*
[24b]*Dipartimento di Fisica, Università di Genova, I-16146 Genova, Italy*
[25]*Indian Institute of Technology Guwahati, Guwahati, Assam 781 039, India*
[26]*Harvard University, Cambridge, Massachusetts 02138, USA*
[27]*Harvey Mudd College, Claremont, California 91711*
[28]*Universität Heidelberg, Physikalisches Institut, Philosophenweg 12, D-69120 Heidelberg, Germany*
[29]*Humboldt-Universität zu Berlin, Institut für Physik, Newtonstraße 15, D-12489 Berlin, Germany*
[30]*Imperial College London, London, SW7 2AZ, United Kingdom*
[31]*University of Iowa, Iowa City, Iowa 52242, USA*
[32]*Iowa State University, Ames, Iowa 50011-3160, USA*
[33]*Johns Hopkins University, Baltimore, Maryland 21218, USA*
[34]*Laboratoire de l'Accélérateur Linéaire, IN2P3/CNRS et Université Paris-Sud 11, Centre Scientifique d'Orsay, Boîte Postale 34, F-91898 Orsay Cedex, France*
[35]*Lawrence Livermore National Laboratory, Livermore, California 94550, USA*
[36]*University of Liverpool, Liverpool L69 7ZE, United Kingdom*
[37]*Queen Mary, University of London, London E1 4NS, United Kingdom*
[38]*University of London, Royal Holloway and Bedford New College, Egham, Surrey TW20 0EX, United Kingdom*
[39]*University of Louisville, Louisville, Kentucky 40292, USA*
[40]*Johannes Gutenberg-Universität Mainz, Institut für Kernphysik, D-55099 Mainz, Germany*

[41]University of Manchester, Manchester M13 9PL, United Kingdom
[42]University of Maryland, College Park, Maryland 20742, USA
[43]University of Massachusetts, Amherst, Massachusetts 01003, USA
[44]Massachusetts Institute of Technology, Laboratory for Nuclear Science, Cambridge, Massachusetts 02139, USA
[45]McGill University, Montréal, Québec Canada H3A 2T8
[46a]INFN Sezione di Milano, I-20133 Milano, Italy
[46b]Dipartimento di Fisica, Università di Milano, I-20133 Milano, Italy
[47]University of Mississippi, University, Mississippi 38677, USA
[48]Université de Montréal, Physique des Particules, Montréal, Québec, Canada H3C 3J7
[49a]INFN Sezione di Napoli, I-80126 Napoli, Italy
[49b]Dipartimento di Scienze Fisiche, Università di Napoli Federico II, I-80126 Napoli, Italy
[50]NIKHEF, National Institute for Nuclear Physics and High Energy Physics, NL-1009 DB Amsterdam, The Netherlands
[51]University of Notre Dame, Notre Dame, Indiana 46556, USA
[52]Ohio State University, Columbus, Ohio 43210, USA
[53]University of Oregon, Eugene, Oregon 97403, USA
[54a]INFN Sezione di Padova, I-35131 Padova, Italy
[54b]Università di Padova, I-35131 Padova, Italy
[55]Laboratoire de Physique Nucléaire et de Hautes Energies, IN2P3/CNRS, Université Pierre et Marie Curie-Paris6, Université Denis Diderot-Paris7, F-75252 Paris, France
[56a]INFN Sezione di Perugia, I-06100 Perugia, Italy
[56b]Dipartimento di Fisica, Università di Perugia, I-06100 Perugia, Italy
[57a]INFN Sezione di Pisa, I-56127 Pisa, Italy
[57b]Dipartimento di Fisica, Università di Pisa, I-56127 Pisa, Italy
[57c]Scuola Normale Superiore di Pisa, I-56127 Pisa, Italy
[58]Princeton University, Princeton, New Jersey 08544, USA
[59a]INFN Sezione di Roma, I-00185 Roma, Italy
[59b]Dipartimento di Fisica, Università di Roma La Sapienza, I-00185 Roma, Italy
[60]Universität Rostock, D-18051 Rostock, Germany
[61]Rutherford Appleton Laboratory, Chilton, Didcot, Oxon OX11 0QX, United Kingdom
[62]CEA, IRFU, SPP, Centre de Saclay, F-91191 Gif-sur-Yvette, France
[63]SLAC National Accelerator Laboratory, Stanford, California 94309 USA
[64]University of South Carolina, Columbia, South Carolina 29208, USA
[65]Southern Methodist University, Dallas, Texas 75275, USA
[66]Stanford University, Stanford, California 94305-4060, USA
[67]State University of New York, Albany, New York 12222, USA
[68]Tel Aviv University, School of Physics and Astronomy, Tel Aviv, 69978, Israel
[69]University of Tennessee, Knoxville, Tennessee 37996, USA
[70]University of Texas at Austin, Austin, Texas 78712, USA
[71]University of Texas at Dallas, Richardson, Texas 75083, USA
[72a]INFN Sezione di Torino, I-10125 Torino, Italy
[72b]Dipartimento di Fisica Sperimentale, Università di Torino, I-10125 Torino, Italy
[73a]INFN Sezione di Trieste, I-34127 Trieste, Italy
[73b]Dipartimento di Fisica, Università di Trieste, I-34127 Trieste, Italy
[74]IFIC, Universitat de Valencia-CSIC, E-46071 Valencia, Spain
[75]University of Victoria, Victoria, British Columbia, Canada V8W 3P6
[76]Department of Physics, University of Warwick, Coventry CV4 7AL, United Kingdom
[77]University of Wisconsin, Madison, Wisconsin 53706, USA

(Received 22 December 2010; published 8 March 2011)

We present measurements of the branching fractions, longitudinal polarization, and direct CP-violation asymmetries for the decays $B^+ \to \rho^0 K^{*+}$ and $B^+ \to f_0(980)K^{*+}$ with a sample of $(467 \pm 5) \times 10^6 B\bar{B}$ pairs collected with the *BABAR* detector at the PEP-II asymmetric-energy e^+e^- collider at the SLAC National Accelerator Laboratory. We observe $B^+ \to \rho^0 K^{*+}$ with a significance of 5.3σ and measure the branching fraction $\mathcal{B}(B^+ \to \rho^0 K^{*+}) = (4.6 \pm 1.0 \pm 0.4) \times 10^{-6}$, the longitudinal polarization

*Now at Temple University, Philadelphia, Pennsylvania 19122, USA
†Also with Università di Perugia, Dipartimento di Fisica, Perugia, Italy
‡Also with Università di Roma La Sapienza, I-00185 Roma, Italy
§Now at University of South Alabama, Mobile, Alabama 36688, USA
‖Also with Università di Sassari, Sassari, Italy

$f_L = 0.78 \pm 0.12 \pm 0.03$, and the CP-violation asymmetry $\mathcal{A}_{CP} = 0.31 \pm 0.13 \pm 0.03$. We observe $B^+ \to f_0(980)K^{*+}$ and measure the branching fraction $\mathcal{B}(B^+ \to f_0(980)K^{*+}) \times \mathcal{B}(f_0(980) \to \pi^+\pi^-) = (4.2 \pm 0.6 \pm 0.3) \times 10^{-6}$ and the CP-violation asymmetry $\mathcal{A}_{CP} = -0.15 \pm 0.12 \pm 0.03$. The first uncertainty quoted is statistical and the second is systematic.

DOI: 10.1103/PhysRevD.83.051101 PACS numbers: 13.25.Hw, 11.30.Er, 12.15.Hh

The study of the branching fractions and angular distributions of B meson decays to hadronic final states without a charm quark probes the dynamics of both the weak and strong interactions. It also plays an important role in understanding CP violation in the quark sector, constraining the Cabibbo-Kobayashi-Maskawa matrix parameters [1] and searching for evidence for physics beyond the standard model [2,3].

The charmless decays $B \to \rho K^*$ proceed through penguin loops and tree processes ($B^+ \to \rho^+ K^{*0}$ is a pure penguin process) to two vector particles (VV). QCD factorization models predict a large longitudinal polarization fraction f_L [of order $(1 - 4m_V^2/m_B^2) \sim 0.9$] for VV decays [4]. However, measurements of penguin-dominated VV decays give f_L as low as $\sim$0.5 [5]. Several attempts to understand the values of f_L within or beyond the standard model have been made [6].

For the $B^+ \to \rho^0 K^{*+}$ branching fraction, Beneke, Rohrer and Yang [2] predict the CP-averaged branching fraction to be $(4.5^{+1.5+3.0}_{-1.3-1.4}) \times 10^{-6}$, while Cheng and Yang [3] quote $(5.5^{+0.6+1.3}_{-0.5-2.5}) \times 10^{-6}$, both based on QCD factorization. The 90% C.L. upper limit $B^+ \to \rho^0 K^{*+}$ branching fraction has been measured to be $<6.1 \times 10^{-6}$ [7].

We report measurements of branching fractions, longitudinal polarizations, and direct CP-violating asymmetries for the decay modes $B^+ \to \rho^0 K^{*+}$ and $B^+ \to f_0(980)K^{*+}$, where ρ^0 and K^{*+} refer to the $\rho^0(770)$ and $K^{*+}(892)$ resonances, respectively. The analysis is based on a data sample of $(467 \pm 5) \times 10^6 B\bar{B}$ pairs, equivalent to an integrated luminosity of 426 fb^{-1}, collected with the *BABAR* detector at the PEP-II asymmetric-energy e^+e^- collider operated at the SLAC National Accelerator Laboratory. The e^+e^- center-of-mass (c.m.) energy is $\sqrt{s} = 10.58$ GeV, corresponding to the $\Upsilon(4S)$ resonance mass (on-resonance data). In addition, 44.4 fb^{-1} of data collected 40 MeV below the $\Upsilon(4S)$ resonance (off-resonance data) are used for background studies. We assume equal production rates of B^+B^- and $B^0\bar{B}^0$ mesons, and charge-conjugate modes are implied throughout [8]. The *BABAR* detector is described in detail in Ref. [9].

The $B^+ \to \rho^0 K^{*+}$ and $B^+ \to f_0(980)K^{*+}$ candidates are reconstructed through the decays of ρ^0 or $f_0(980) \to \pi^+\pi^-$, $K^{*+} \to K^0_S\pi^+$ or $K^{*+} \to K^+\pi^0$, with $K^0_S \to \pi^+\pi^-$ and $\pi^0 \to \gamma\gamma$. The differential decay rate for $B^+ \to \rho^0 K^{*+}$, after integrating over the angle between the decay planes of the vector mesons, for which the acceptance is nearly uniform, is proportional to

$$\frac{1 - f_L}{4} \sin^2\theta_{K^{*+}} \sin^2\theta_{\rho^0} + f_L \cos^2\theta_{K^{*+}} \cos^2\theta_{\rho^0}, \quad (1)$$

where $\theta_{K^{*+}}$ (θ_{ρ^0}) is the helicity angle of the K^{*+} (ρ^0), defined as the angle between the daughter K (π^+) momentum and the direction opposite to the B meson momentum in the K^{*+} (ρ^0) rest frame [10]. The direct CP-violating asymmetry $\mathcal{A}_{CP}$ is defined as $\mathcal{A}_{CP} = (\Gamma^- - \Gamma^+)/(\Gamma^- + \Gamma^+)$, where $\Gamma^\pm = \Gamma(B^\pm \to f^\pm)$ is the decay width for a given charged final state $f^\pm$.

We apply the same selection criteria for ρ^0 and $f_0(980)$ candidates. The charged particles from the K^{*+} and ρ^0 decays are required to have a transverse momentum relative to the beam axis greater than 0.05 GeV/c. The particles are identified as either charged pions or kaons by measurement of the energy loss in the tracking detectors, the number of photons recorded by the ring-imaging Cherenkov detector and the corresponding Cherenkov angle. These measurements are combined with information from the electromagnetic calorimeter and the instrumented magnetic-flux return detector, where appropriate, to reject electrons, muons, and protons.

The K^0_S candidates are required to have a mass within 0.01 GeV/c^2 of the nominal K^0_S mass [8], a decay vertex separated from the B meson decay vertex by at least 20 times the uncertainty in the measurement of the separation of the vertex positions, a flight distance in the direction transverse to the beam axis of at least 0.3 cm, and the cosine of the angle between the line joining the B and K^0_S decay vertices and the K^0_S momentum greater than 0.999.

In the laboratory frame, the energy of each photon from the π^0 candidate must be greater than 0.03 GeV, the π^0 energy must exceed 0.25 GeV, and the reconstructed π^0 invariant mass is required to be in the range $0.12 \leq m_{\gamma\gamma} \leq 0.15$ GeV/c^2. After selection, the π^0 candidate's mass is constrained to its nominal value [8].

We require the invariant mass of the K^{*+} and ρ^0 candidates to satisfy $0.792 < m_{K\pi} < 0.992$ GeV/c^2 and $0.52 < m_{\pi^+\pi^-} < 1.05$ GeV/c^2, respectively. A B meson candidate is formed from the K^{*+} and ρ^0 candidates, with the condition that the K^{*+} and ρ^0 candidates originate from the interaction region and the χ^2 of the B meson vertex fit is less than 100. We require that there is at least one additional charged track in the event and create a vertex for a second B meson from all remaining charged tracks and neutral clusters that are consistent with originating from the interaction region.

The B meson candidates are characterized kinematically by the energy difference $\Delta E = E_B^* - \sqrt{s}/2$ and the beam energy-substituted mass $m_{\rm ES} = [(s/2 + \mathbf{p}\cdot\mathbf{p}_B)^2/E^2 - \mathbf{p}_B^2]^{1/2}$, where $(E, \mathbf{p})$ and $(E_B, \mathbf{p}_B)$ are the four-momenta of the $\Upsilon(4S)$ and B meson candidate in the laboratory frame, respectively, and the asterisk denotes the c.m. frame. The event sample is taken from the region $|\Delta E| < 0.10$ GeV and $5.255 \le m_{\rm ES} \le 5.289$ GeV/c^2. The extended $m_{\rm ES}$ range ensures the shape of the background distribution is properly modeled. Sideband events, outside the region $|\Delta E| \le 0.07$ GeV and $5.270 \le m_{\rm ES} \le 5.289$ GeV/c^2, are used to characterize the background and cross-check the Monte Carlo (MC) background simulations [11].

We suppress the background from B mesons decaying to charm by forming the invariant mass m_D from combinations of two or three out of the four daughter particles' four-momenta. The event is rejected if $1.835 < m_D < 1.895$ GeV/c^2 and the charge and particle type of the tracks are consistent with a known decay from a D meson [8]. Finally, to reduce the background and to avoid the region where the reconstruction efficiency falls off rapidly for low momentum tracks, we require the cosines of the helicity angles of the K^{*+} and ρ^0 candidates to satisfy $\cos\theta_{K^{*+}} \le 0.92$ and $|\cos\theta_{\rho^0}| \le 0.95$, respectively.

To reject the background consisting of light-quark $q\bar{q}$ ($q = u,\ d,\ s,\ c$) continuum events, we require $|\cos\theta_T| < 0.85$, where θ_T is the angle, in the c.m. frame, between the thrust axis of the B meson and that formed from the other tracks and neutral clusters in the event. Signal events have an approximately uniform distribution in $|\cos\theta_T|$, while $q\bar{q}$ continuum events peak at 1.

After the application of the selection criteria, the average number of $\rho^0 K^{*+}$ candidates per event with $K^{*+} \to K_S^0\pi^+$ in signal MC simulations is 1.14 (1.03) for fully longitudinally (transversely) polarized decays. The candidate with the smallest fitted decay vertex χ^2 is chosen. Up to 2.1% (1.0%) of longitudinally (transversely) polarized MC signal events are misreconstructed, with one or more tracks originating from the other B meson in the event. For $\rho^0 K^{*+}$ with $K^{*+} \to K^+\pi^0$, the average number of candidates per event is 1.20 (1.08) and the fraction of misreconstructed candidates is 5.9% (2.7%) for fully longitudinally (transversely) polarized decays. For $f_0(980)K^{*+}$, the number of candidates per event and the fraction of misreconstructed events are 1.02 (1.06) and 9.1% (13.8%) for decays with $K^{*+} \to K_S^0\pi^+$ ($K^{*+} \to K^+\pi^0$). The ρ^0 and K^{*+} masses and widths in the MC simulation are taken from Ref. [8], and we use the measured $f_0(980)$ line shape from Ref. [12].

A neural net discriminant is used to provide additional separation between signal and $q\bar{q}$ continuum. It is constructed from six variables calculated in the c.m. frame: the polar angles of the B meson momentum vector and the B meson thrust axis with respect to the beam axis, the angle between the B meson thrust axis and the thrust axis of the rest of the event, the ratio of the second- and zeroth-order momentum-weighted polynomial moments of the energy flow around the B meson thrust axis [13], the flavor of the other B meson as reported by a multivariate tagging algorithm [14], and the boost-corrected proper-time difference between the decays of the two B mesons divided by its variance. The discriminant is trained using MC for the signal, and $q\bar{q}$ continuum MC and off-resonance data for the background.

We define an extended likelihood function to be used in an unbinned maximum likelihood (ML) fit as

$$\mathcal{L} = \frac{1}{N!}\exp\Big(-\sum_j n_j\Big)\prod_{i=1}^{N}\Big[\sum_j n_j \mathcal{P}_j(\vec{x}_i;\vec{\alpha}_j)\Big], \qquad (2)$$

where the likelihood $\mathcal{L}_i$ for each event candidate i is the sum of $n_j\mathcal{P}_j(\vec{x}_i;\vec{\alpha}_j)$ over hypotheses j: two signal modes $\rho^0 K^{*+}$ and $f_0(980)K^{*+}$ (including misreconstructed signal candidates); $q\bar{q}$ continuum background; and nine $B\bar{B}$ backgrounds as discussed below. $\mathcal{P}_j(\vec{x}_i;\vec{\alpha}_j)$ is the product of the probability density functions (PDFs) for hypothesis j evaluated for the i-th event's measured variables $\vec{x}_i$. The number of events for hypothesis j is denoted by n_j, and N is the total number of events in the sample. The quantities $\vec{\alpha}_j$ represent parameters to describe the expected distributions of the measured variables for each hypothesis j. Each discriminating variable $\vec{x}_i$ in the likelihood function is modeled with a PDF, where the parameters $\vec{\alpha}_j$ are extracted from MC simulation, off-resonance data, or ($m_{\rm ES}$, ΔE) sideband data. The seven variables $\vec{x}_i$ used in the fit are $m_{\rm ES}$, ΔE, the neural net output, $m_{\pi^+\pi^-}$, $m_{K\pi}$, the absolute cosine of the helicity angle of the $\rho^0/f_0(980)$ candidate, and the cosine of the helicity of the K^{*+} candidate. Since most of the linear correlations among the fit variable distributions are found to be about 1%, with a maximum of 11%, we take each $\mathcal{P}_j$ to be the product of the PDFs for the separate variables.

The decays $B^+ \to \bar{D}^0(\to K_S^0\pi^+\pi^-)\pi^+$ and $B^+ \to \bar{D}^0(\to K^+\pi^0\pi^-)\pi^+$ have large branching fractions and a topology similar to the decays under consideration. They are used as calibration channels. We apply the same selection criteria as described above except that the neural net is trained on the MC simulated data for the calibration channel under consideration; the ΔE range is reduced to $|\Delta E| < 0.08$ GeV; the $m_{K\pi}$ and $m_{\pi^+\pi^-}$ mass criteria are replaced with a mass range $1.8445 < m_{\bar{D}^0} < 1.8845$ GeV/c^2; and no D meson veto is applied. We use the selected data to verify that the ML fit is performing correctly and that the MC is simulating the neural net, ΔE, and $m_{\rm ES}$ distributions.

Backgrounds from $B\bar{B}$ decays involving charmed mesons are effectively suppressed by applying the veto on the D meson mass described above. The $B\bar{B}$ backgrounds that remain after the event selection criteria have been applied are identified and modeled using MC simulation.

We categorize the $B\bar{B}$ backgrounds in the ML fit into nine main groups. Two groups represent decays where either a K^{*+} or a $\rho^0/f_0(980)$ is falsely reconstructed. Four groups represent nonresonant final states $\pi^+\pi^-K^{*+}$, $\rho^0(K\pi)^+$, $\pi^+\pi^-(K\pi)^+$, and $f_0(980)(K\pi)^+$, where $(K\pi)^+$ stands for $K^0_S\pi^+$ or $K^+\pi^0$. The decays $B^0 \to \eta' K^0_S$ and $B^+ \to \eta' K^+$ peak at high $\cos\theta_{K^{*+}}$ and are assigned their own category. We allow for decays from higher mass $K^*_0(1430)$ states. All remaining $B\bar{B}$ background decays that are not accounted for by the above groups are assigned to a dominant remainder group.

The invariant mass distributions in the ML fit are modeled with relativistic Breit-Wigner functions for the K^{*+} and $f_0(980)$, together with a polynomial of order up to four for the smoothly varying distribution of misreconstructed candidates. Following Ref. [15], a modified relativistic Breit-Wigner function is used for the ρ^0 meson. The $K^*_0(1430)$ is modeled with the LASS parametrization, which consists of the $K^*_0(1430)$ resonance together with an effective-range nonresonant component [16]. For the signal, the distributions of the cosine of the helicity angles are described by Eq. (1) multiplied by a polynomial acceptance function that corrects for changes in efficiency as a function of helicity angle. The correction also accounts for the reduction in efficiency at helicity near 0.78 introduced indirectly by the criteria used to veto D mesons. For backgrounds, the cosine of the helicity angle distribution is modeled with a polynomial. The neural net distributions are modeled using either an empirical nonparametric function [17] or a histogram. For $m_{\rm ES}$, an asymmetric Gaussian is used for the signal; the function $x\sqrt{1-x^2}\exp[-\xi(1-x^2)]$ with $x = m_{\rm ES}/E^*_B$ and ξ a free parameter [18] is used for $q\bar{q}$ continuum and $B\bar{B}$ backgrounds; and a combination of an asymmetric Gaussian with a polynomial is used for all other hypotheses. For ΔE, two Gaussians are used for signal and polynomials for all other hypotheses.

We simultaneously fit for the branching fractions $\mathcal{B}$, $\mathcal{A}_{CP}$, and f_L (for $B^+ \to \rho^0 K^{*+}$ only). We allow the yields for all hypotheses to float except for $\rho^0(K\pi)^+$ and $f_0(980)(K\pi)^+$ which are fixed to their predicted MC yields, assuming a branching fraction of 1×10^{-6}. The predicted yields for the fixed modes are less than one event. The PDF parameters ξ for $m_{\rm ES}$, the slope of the ΔE distribution, and the polynomial coefficients and normalizations describing the mass and helicity angle distributions are allowed to vary for the $q\bar{q}$ continuum and $B\bar{B}$ remainder groups. We validate the fitting procedure and obtain the sizes of potential biases on the fit results by applying the fit to ensembles of simulated experiments using the extracted fitted yields from data. The observed fit biases in the MC samples are subtracted from the fitted yields measured in the data.

The results of the ML fits are summarized in Table I, where we assume a branching fraction of 100% for $f_0(980) \to \pi^+\pi^-$. For decays with $K^{*+} \to K^0_S\pi^+$ ($K^{*+} \to K^+\pi^0$), the event sample is 7444 (12 867), with 5959 ± 96 ($10\,727 \pm 122$) fitted $q\bar{q}$ continuum events and 1266 ± 81 (1451 ± 129) events in the $B\bar{B}$ background remainder group. The signal significance S is defined as $S = \sqrt{2\Delta \ln \mathcal{L}}$, where $\Delta \ln \mathcal{L}$ is the change in log-likelihood from the maximum value to the value when the number of signal events is set to zero, corrected for systematic errors by convolving the likelihood function with a Gaussian distribution with a variance equal to the total systematic error defined below. The linear correlation coefficient between the $\rho^0 K^{*+}$ and $f_0(980)K^{*+}$ branching fractions is 0.25.

Figures 1 and 2 show the projections of the fits onto $m_{\rm ES}$, ΔE, the masses, and the cosines of the helicity angles for decays with $K^{*+} \to K^0_S\pi^+$ and $K^{*+} \to K^+\pi^0$, respectively. The candidates in the figures are subject to a requirement on the probability ratio $\mathcal{P}_{\rm sig}/(\mathcal{P}_{\rm sig} + \mathcal{P}_{\rm bkg}) > 0.9$, where $\mathcal{P}_{\rm sig}$ and $\mathcal{P}_{\rm bkg}$ are the signal and total background probabilities, respectively, computed without the use of the variable plotted.

The systematic errors on the yields and branching fractions arise from the PDFs, fit biases, $f_0(980)$ parameters, interference, $B\bar{B}$ background yields, and efficiencies. The PDF uncertainties are calculated by varying the PDF parameters that are held fixed in the original fit by their errors, taking into account correlations. The uncertainty from the fit bias includes its statistical uncertainty from the simulated experiments and half of the correction itself,

TABLE I. Results for the measured B decays: signal yield Y (corrected for fit bias) and its statistical uncertainty, reconstruction efficiency (%), daughter branching fraction product $\Pi\mathcal{B}_i$(%) [8], significance S (with statistical and systematic uncertainties included), branching fraction $\mathcal{B}$, 90% C.L. upper limit (for modes with $S < 6\sigma$), longitudinal polarization f_L and CP-violating asymmetry A_{CP}.

Mode	Y	ϵ(%)	$\Pi\mathcal{B}_i$(%)	$S(\sigma)$	$\mathcal{B}(\times 10^{-6})$	UL$(\times 10^{-6})$	f_L	$\mathcal{A}_{CP}$
$B^+ \to \rho^0 K^{*+}$				5.3	$4.6 \pm 1.0 \pm 0.4$	6.0	$0.78 \pm 0.12 \pm 0.03$	$0.31 \pm 0.13 \pm 0.03$
$K^{*+} \to K^0_S\pi^+$	85 ± 24	17.1	23.1	4.1	$4.6 \pm 1.2 \pm 0.5$	6.4	$0.74 \pm 0.13 \pm 0.03$	$0.25 \pm 0.14 \pm 0.03$
$K^{*+} \to K^+\pi^0$	67 ± 31	9.9	33.3	3.3	$4.4 \pm 2.0 \pm 0.5$	7.1	$0.94 \pm 0.27 \pm 0.03$	$0.59 \pm 0.31 \pm 0.03$
$B^+ \to f_0(980)K^{*+}$				9.0	$4.2 \pm 0.6 \pm 0.3$			$-0.15 \pm 0.12 \pm 0.03$
$K^{*+} \to K^0_S\pi^+$	69 ± 14	17.9	23.1	6.0	$3.6 \pm 0.7 \pm 0.3$			$-0.34 \pm 0.16 \pm 0.03$
$K^{*+} \to K^+\pi^0$	91 ± 20	11.3	33.3	6.8	$5.2 \pm 1.0 \pm 0.3$			$0.14 \pm 0.12 \pm 0.03$

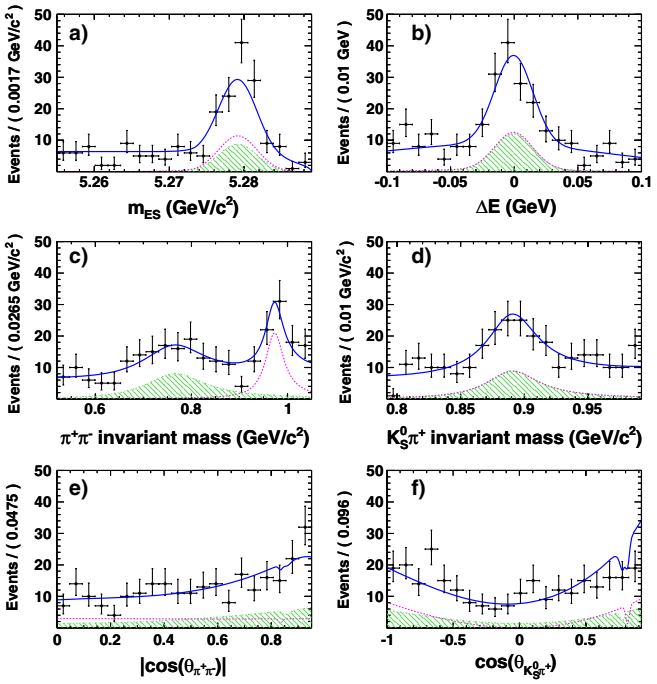

FIG. 1 (color online). Projections of the multidimensional fit onto (a) $m_{\rm ES}$, (b) ΔE, (c) $\pi^+\pi^-$ mass, (d) $K^0_S\pi^+$ mass, (e) $|\cos\theta_{\pi^+\pi^-}|$, and (f) $\cos\theta_{K^0_S\pi^+}$ for modes with $K^{*+} \to K^0_S\pi^+$. The points with error bars show the data; the solid line shows signal-plus-background; the hatched [green] area is the $\rho^0 K^{*+}$ signal; and the dashed [red] line is the $f_0(980)K^{*+}$ signal.

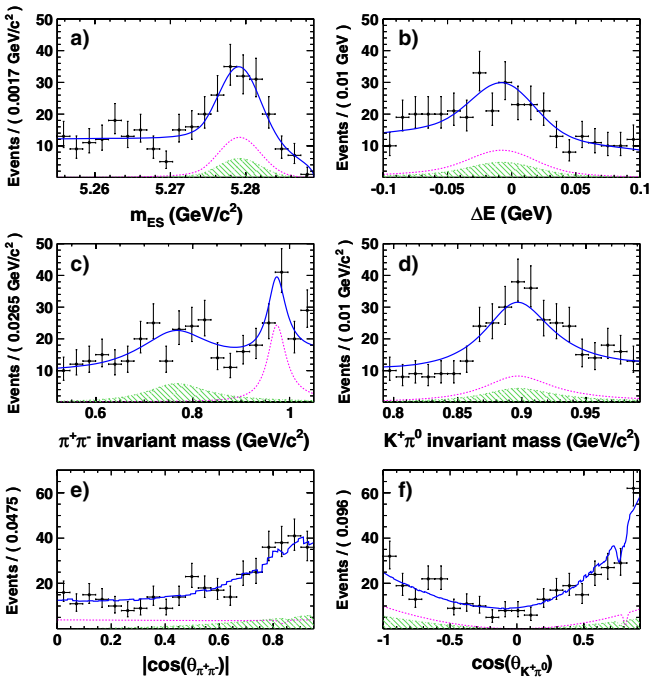

FIG. 2 (color online). Projections of the multidimensional fit onto (a) $m_{\rm ES}$, (b) ΔE, (c) $\pi^+\pi^-$ mass, (d) $K^+\pi^0$ mass, (e) $|\cos\theta_{\pi^+\pi^-}|$, and (f) $\cos\theta_{K^+\pi^0}$ for modes with $K^{*+} \to K^+\pi^0$. The figure uses the same projection criteria and legend as Fig. 1.

added in quadrature. We allow for uncertainties in the $f_0(980)$ line shape by performing a separate fit with the $f_0(980)$ mean and width as additional free parameters. The effect of possible interference between the $f_0(980)$ and ρ^0 is estimated by adding the $f_0(980)$ and ρ^0 amplitudes together with a varying phase difference and using half the maximum change in the yield as an uncertainty. We test for the presence of a scalar $f_0(600)$ (or σ) by adding it to our model, using the mass and width reported in Ref. [19]. The contribution of the $B\bar{B}$ backgrounds to the error is calculated by performing an ensemble of fits to the data where backgrounds are either removed from the fit (for those categories with a fitted number of events consistent with zero), allowed to float (for the fixed backgrounds) or fixed to the expected number of events calculated from MC. The error is calculated as half the difference between the default fit and the maximum deviation seen in the ensemble of fits. Finally, the uncertainty on the longitudinal polarization affects the calculated yield efficiency. All these errors are additive in nature and affect the significance of the branching fraction results. We assume the sources of the uncertainties that contribute to the additive errors are uncorrelated when combined to form the overall branching fractions. The PDF parameter uncertainty contributes up to 0.4 signal events to the systematic error and the fit bias between 2.4 and 0.8 events, depending on the signal mode. We see no evidence for the $f_0(600)$ state. The $f_0(980)$ line shape and interference account for up to 0.8 and 2.0 events, respectively. The overall systematic error is dominated by the uncertainty in the $B\bar{B}$ backgrounds and, for $\rho^0 K^{*+}$, the systematic error on f_L. The total additive systematic error on the $B^+ \to \rho^0 K^{*+}$ signal yield is 9.4 and 6.7 events for $K^{*+} \to K^0_S\pi^+$ and $K^{*+} \to K^+\pi^0$, respectively, and for $B^+ \to f_0(980)K^{*+}$ it is 4.4 and 1.3 events, respectively.

Multiplicative uncertainties include reconstruction efficiency uncertainties from tracking (0.8% per track added linearly), charged particle identification (1.1% per track added linearly), π^0 identification (3.0%), K^0_S identification (1.0%), track multiplicity (1.0%), the number of $B\bar{B}$ pairs (1.1%), and MC signal statistics (0.2%). The total multiplicative branching fraction systematic error is 4.5% and 5.3% for decays with $K^{*+} \to K^0_S\pi^+$ and $K^{*+} \to K^+\pi^0$, respectively. The multiplicative uncertainties for both submodes are correlated. The majority of the systematic uncertainties on f_L and $\mathcal{A}_{CP}$ cancel, and the error is dominated by the uncertainty on the PDF parameters (0.02). The uncertainty due to the dependence of the reconstruction efficiency on the charge of the kaon is estimated from MC to be 0.005. The total systematic is calculated to be ± 0.03 for all modes.

In summary, we observe $B^+ \to \rho^0 K^{*+}$ with a significance of 5.3σ. We measure the branching fraction $\mathcal{B}(B^+ \to \rho^0 K^{*+}) = (4.6 \pm 1.0 \pm 0.4) \times 10^{-6}$, the longitudinal polarization $f_L = 0.78 \pm 0.12 \pm 0.03$, and the

CP-violating asymmetry $\mathcal{A}_{CP} = 0.31 \pm 0.13 \pm 0.03$. We observe $B^+ \to f_0(980)K^{*+}$ and measure the branching fraction $\mathcal{B}(B^+ \to f_0(980)K^{*+}) \times \mathcal{B}(f_0(980) \to \pi^+\pi^-) = (4.2 \pm 0.6 \pm 0.3) \times 10^{-6}$ and the CP-violating asymmetry $\mathcal{A}_{CP} = -0.15 \pm 0.12 \pm 0.03$. The $B^+ \to \rho^0 K^{*+}$ branching fraction is compatible with theoretical predictions [2,3].

We are grateful for the excellent luminosity and machine conditions provided by our PEP-II colleagues, and for the substantial dedicated effort from the computing organizations that support *BABAR*. The collaborating institutions wish to thank SLAC for its support and kind hospitality. This work is supported by DOE and NSF (USA), NSERC (Canada), CEA and CNRS-IN2P3 (France), BMBF and DFG (Germany), INFN (Italy), FOM (The Netherlands), NFR (Norway), MES (Russia), MICIIN (Spain), and STFC (United Kingdom). Individuals have received support from the Marie Curie EIF (European Union), the A. P. Sloan Foundation (USA) and the Binational Science Foundation (USA-Israel).

[1] N. Cabibbo, Phys. Rev. Lett. **10**, 531 (1963); M. Kobayashi and T. Maskawa, Prog. Theor. Phys. **49**, 652 (1973).
[2] M. Beneke, J. Rohrer, and D. S. Yang, Nucl. Phys. **B774**, 64 (2007).
[3] H. Y. Cheng and K. C. Yang, Phys. Rev. D **78**, 094001 (2008); **79**, 039903(E) (2009).
[4] A. Ali *et al.*, Z. Phys. C **1**, 269 (1979); M. Suzuki, Phys. Rev. D **66**, 054018 (2002).
[5] K.-F. Chen *et al.* (Belle Collaboration), Phys. Rev. Lett. **94**, 221804 (2005); B. Aubert *et al.* (*BABAR* Collaboration), Phys. Rev. Lett. **98**, 051801 (2007); Phys. Rev. Lett. **99**, 201802 (2007).
[6] A. Kagan, Phys. Lett. B **601**, 151 (2004); C. Bauer *et al.*, Phys. Rev. D **70**, 054015 (2004); P. Colangelo *et al.*, Phys. Lett. B **597**, 291 (2004); M. Ladisa *et al.*, Phys. Rev. D **70**, 114025 (2004); H.-n. Li and S. Mishima, Phys. Rev. D **71**, 054025 (2005); M. Beneke *et al.*, Phys. Rev. Lett. **96**, 141801 (2006).
[7] B. Aubert *et al.* (*BABAR* Collaboration), Phys. Rev. Lett. **97**, 201801 (2006).
[8] C. Amsler *et al.* (Particle Data Group) Phys. Lett. B **667**, 1 (2008).
[9] B. Aubert *et al.* (*BABAR* Collaboration), Nucl. Instrum. Methods Phys. Res., Sect. A **479**, 1 (2002).
[10] G. Kramer and W. F. Palmer, Phys. Rev. D **45**, 193 (1992).
[11] S. Agostinelli *et al.* (GEANT Collaboration), Nucl. Instrum. Methods Phys. Res., Sect. A **506**, 250 (2003).
[12] E. M. Aitala *et al.*, Phys. Rev. Lett. **86**, 765 (2001).
[13] B. Aubert *et al.* (*BABAR* Collaboration), Phys. Rev. D **70**, 032006 (2004).
[14] B. Aubert *et al.* (*BABAR* Collaboration), Phys. Rev. Lett. **94**, 161803 (2005).
[15] G. J. Gounaris and J. J. Sakurai, Phys. Rev. Lett. **21**, 244 (1968).
[16] D. Aston *et al.* (LASS Collaboration), Nucl. Phys. **B296**, 493 (1988).
[17] K. S. Kramer, Comput. Phys. Commun. **136**, 198 (2001).
[18] H. Albrecht *et al.* (ARGUS Collaboration), Phys. Lett. B **241**, 278 (1990).
[19] H. Muramatsu *et al.* (CLEO Collaboration), Phys. Rev. Lett. **89**, 251802 (2002).